ORIGINAL ARTICLE

The Role of Secondary Cyclones and Cyclone Families for the North Atlantic Storm Track and Clustering over Western Europe

Matthew D. K. Priestley[1*] | Helen F. Dacre[1] | Len C. Shaffrey[2] | Sebastian Schemm[3] | Joaquim G. Pinto[4]

[1]Department of Meteorology, University of Reading, Reading, UK

[2]NCAS, Department of Meteorology, University of Reading, Reading, UK

[3]Institute for Atmospheric and Climate Science,ETH Zürich, Zürich, Switzerland

[4]Institute of Meteorology and Climate Research, Karlsruhe Institute of Technology, Karlsruhe, Germany

Correspondence
Matthew D. K. Priestley, College of Engineering, Mathematics and Physical Sciences, University of Exeter, Exeter, UK
Email: m.priestley@exeter.ac.uk

Present address
College of Engineering, Mathematics and Physical Sciences, University of Exeter, Exeter, UK

Funding information
NERC SCENARIO DTP co-funded by Aon Impact Forecasting (NE/L002566/1). AXA Research Fund. ERA4CS WINDSURFER project.

Secondary cyclones are those that form in association with a pre-existing primary cyclone with this commonly being along a trailing cold front. In previously studied cases they have been shown to cause extreme damage across Europe, particularly when multiple cyclones track over the same location in rapid succession (known as cyclone clustering). To determine the dynamical relationship between primary and secondary cyclones over the North Atlantic, a frontal identification algorithm is partnered with a cyclone identification method to objectively identify secondary cyclones in 35 extended winter periods using re-analysis data. Cyclones are grouped into 'cyclone families' consisting of a single primary cyclone and one or more secondary cyclones. This paper aims to quantify the differences between secondary and primary cyclones over the North Atlantic, and how cyclone families contribute to episodes of cyclone clustering across western Europe.

Secondary cyclones are shown to occur most frequently in the central and eastern North Atlantic, whereas primary cyclones are commonly found over the western North Atlantic. Cyclone families have their strongest presence over the North Atlantic Ocean and contribute more than 50%

of cyclones over the main North Atlantic storm track. A final category, Solo cyclones, which are not associated with cyclogenesis on any connected fronts, are most commonly identified over continental regions and also the Mediterranean Sea. Primary cyclones are associated with the development of an environment that is favourable for Secondary cyclone growth. Enhanced Rossby wave breaking following the primary cyclone development leads to an increase of the upper-level jet speed and a decrease in low-level stability. Secondary cyclogenesis commonly occurs in this region of anomalously low stability, close to the European continent.

During periods of cyclone clustering, secondary cyclones are responsible for approximately 50% of the total number of cyclones. The increase in jet speed and decrease in static stability initiated by the Primary cyclones acts to concentrate the genesis region of secondary cyclones and direct the cyclones that form along a similar track. While there is an increase in secondary cyclogenesis rate near to western Europe during periods of European clustering, the basin-wide secondary cyclogenesis rate decreases during these periods. Thus the large-scale environment redistributes secondary cyclones during periods of clustering rather than increases the total number of secondary cyclones.

KEYWORDS
Secondary Cyclone, Cyclone Family, Clustering, Cyclogenesis, Windstorm

1 | INTRODUCTION

The original conceptual model for extratropical cyclones is the *Norwegian Model* (Bjerknes and Solberg, 1922), which describes how cyclones form and develop throughout their lifetime. The Norwegian model also describes how "cyclone families" can form along the polar front with each successive cyclone forming slightly to the south and west of the one preceding it. This phenomena of cyclone families and specifically cyclogenesis along fronts has been studied and observed in previous case studies (e.g. Rivals et al., 1998; Chaboureau and Thorpe, 1999), with cyclones forming on the trailing fronts of pre-existing cyclones commonly being called *"Secondary"* cyclones.

Secondary cyclones often develop explosively and have a tendency to cause large amounts of damage, such as the Great Storm of 1987 (Hoskins and Berrisford, 1988), Storms Lothar and Martin in 1999 (Pearce et al., 2001; Wernli et al., 2002), and also Kyrill in January 2007 (Ludwig et al., 2015). These secondary cyclones tend to form from frontal wave instabilities along fronts associated to a pre-existing cyclone (often termed *Primary* cyclones), however, in some cases (~ 50%) these frontal wave instabilities do not develop into cyclones (Parker, 1998), making secondary cyclones difficult to forecast. *Cyclone families* are made up of these primary and any subsequent secondary cyclones.

Secondary and Primary cyclones can be very different in terms of their formation mechanisms. The general formation mechanisms of primary cyclones is well understood as these systems commonly form through baroclinic instability that occurs via the interaction of Rossby waves (Hoskins et al., 1985). With regards to the North Atlantic storm track, this cyclogenesis often occurs near the coast of the North American continent and arises from the strong temperature gradients provided by the SST gradient of the Gulf Stream and the contrasting temperatures of the North American continent (Brayshaw et al., 2009, 2011). For the formation mechanism of secondary cyclones it has been shown that there are many more processes contributing to wave growth.

The theoretical understanding for frontal wave growth comes from Schär and Davies (1990) and Joly and Thorpe (1990) who describe how a potential temperature (θ) or potential vorticity (PV) anomaly along a frontal feature can generate frontal instability and hence wave growth. The analytical model of Bishop and Thorpe (1994a,b) predicted that frontal wave growth was very unlikely for stretching/deformation rates above 0.6-0.8$\times 10^{-5}$ s^{-1}, something which was later confirmed by Schemm and Sprenger (2015). Dacre and Gray (2006) demonstrated that a relaxation of the frontal strain following the generation of the PV/θ was crucial for the generation of individual frontal waves, and summarised the process as follows: a deformation flow along the front drives upward motion which results in latent heat release and forms a PV anomaly strip. This deformation then relaxes, causing a breakdown of the PV strip into smaller anomalies, which may then develop further via interaction with an upper-level wave, this being consistent with Type C cyclogenesis (Plant et al., 2003). This further development of secondary cyclones is not guaranteed (Parker, 1998) with many other contributing factors modulating further growth such as frontal shear (Chaboureau and Thorpe, 1999), latent heat release (Uccellini et al., 1987; Hoskins and Berrisford, 1988; Kuo et al., 1995; Plant et al., 2003), friction in the boundary layer (Adamson et al., 2006), and coastal frontogenesis (Miller, 1946; Bell and Bosart, 1989; Gyakum et al., 1996).

There have been previous attempts to identify secondary cyclogenesis occurring on fronts. The key requirement for identifying these events is the presence of a pre-existing synoptic scale front. There are two main methods for identifying fronts in gridded meteorological data. The first is a thermodynamic method that uses a low-level thermal gradient (commonly equivalent potential temperature) to identify frontal features. This method is mainly based on the framework presented by Hewson (1998) and has been used in a number of studies for the purpose of identifying synoptic-scale fronts (Berry et al., 2011; Catto and Pfahl, 2013; Schemm et al., 2018). A second method of identifying fronts is based on the directional shift and acceleration of the 10-metre wind, as described by Simmonds et al. (2012). This method has also been used in other studies (Papritz et al., 2014). These two methods were compared by Hope et al. (2014) and Schemm et al. (2015). The methods were found to be consistent by Hope et al. (2014), however, Schemm et al. (2015) found the thermodynamic method much better suited to fronts in strongly baroclinic situations (i.e. mid-latitude weather systems), with the wind method being more suited to regions of strong convergence or wind shear, and also for elongated, meridionally oriented fronts.

Schemm and Sprenger (2015) used the thermodynamic method to identify synoptic fronts and the cyclone identification and tracking methodology of Wernli and Schwierz (2006) for finding the cyclogenesis associated with them. This study found that approximately 8-16% of all cyclogenesis events in the western North Atlantic were secondary cyclone events in the December, January, February (DJF) period of 35 winter seasons (1979/80-2013/14), and this was slightly lower at 6-10% in the central North Atlantic. Schemm and Sprenger (2015) also showed how secondary cyclones in the eastern North Atlantic were associated with neutral to negative anomalies in low-level static stability surrounding the cyclone at the time of genesis, consistent with Wang and Rogers (2001) and Dacre and Gray (2009), however, they did not investigate the evolution of the environment surrounding secondary cyclones prior or after genesis. A follow up study by Schemm et al. (2018) found that the tracks of secondary cyclones tended to be located more in the central and eastern parts of the North Atlantic ocean (their figure 5b) and not above the Gulf stream, as would be expected when looking at all cyclones (Hoskins and Hodges, 2002). The identified secondary cyclones in Schemm et al. (2018) make up more than 20% of all cyclones in the central and eastern North Atlantic during DJF. Despite the comprehensive analysis of secondary cyclones by Schemm and Sprenger (2015) and Schemm et al. (2018) they did not objectively identify and compare the related primary cyclones, or quantify any differences in their preferential locations of genesis, track, and lysis.

Extratropical cyclones have been shown to cluster across western Europe (Mailier et al., 2006; Vitolo et al., 2009; Pinto et al., 2014; Priestley et al., 2017b,a), whereby many more cyclones impact a particular geographic region than one would normally expect. Economou et al. (2015) hypothesised that there are three main reasons as to why extratropical cyclones may cluster across the North Atlantic. Firstly, purely by chance. Secondly, through modulation by large-scale atmospheric patterns, such as the North Atlantic Oscillation (NAO). And finally, through a dependence between successive cyclones (i.e. cyclone families). Mailier et al. (2006) and Economou et al. (2015) both showed how the phase of the NAO was associated with a large amount of the variability of clustering across in the North Atlantic. Walz et al. (2018) further highlighted the importance of the phase of the NAO, but also the East Atlantic (EA), and Scandinavian (SCA) patterns in playing a role in modulating the inter-annual variability of serial clustering. The presence of cyclone families during periods of clustering was first highlighted by Pinto et al. (2014), and also in the case study of the 2013/2014 winter season in the UK by Priestley et al. (2017a). Both of these periods were accompanied by a strong and zonally extended jet that was flanked by Rossby wave breaking (RWB) on either flank, steering intense cyclones and cyclone families downstream toward Europe (see also Hanley and Caballero, 2012; Gõmara et al., 2014; Messori and Caballero, 2015). It has yet to be established what causes the increase in cyclone numbers during periods of clustering and whether secondary cyclogenesis plays a relatively more important role.

In this study some of the gaps in the literature presented above are addressed. Particularly identifying the differences between secondary and primary cyclones in the North Atlantic and how secondary cyclones, and their associated cyclone families, contribute to periods of clustering across western Europe. The questions to be answered are as follows:

1. What is the spatial relationship in the genesis and track density of Primary and Secondary cyclones in the North Atlantic?
2. How do the upper and lower level environments evolve during the formation of the Primary and Secondary cyclones?
3. To what extent do Secondary cyclones contribute to the increase in the number of cyclones during periods of clustering that impact western Europe?

This paper is laid out as follows. In section 2 the data and methodology used in the study is presented. Following this results are discussed in section 3. This will start with a climatological discussion of the track/genesis/lysis densities of the different classes of cyclones, question 1 will be addressed in sections 3.1 and 3.2 respectively. Following this the role of the upper-level environment in cyclogenesis posed by question 2 is addressed in section 3.3. Finally, a discussion of the role of secondary cyclones on clustering will follow in 3.4, with question 3 being addressed. In section 4 the key findings are discussed and summarised.

2 | DATA AND METHODOLOGY

2.1 | Dataset

For all of the analysis, the European Centre for Medium-range Weather Forecasts (ECMWF) ERA-Interim re-analysis is used (Dee et al., 2011). The extended winter period of November, December, January, and February (NDJF) from the season of 1979/1980 to 2014/2015 inclusive is used. The horizontal resolution of ERA-Interim is T255 (~80km mid-latitudes), with 60 vertical levels, and 6-hourly temporal resolution.

2.2 | Cyclone and Front Identification

To identify and track extratropical cyclones we use the methodology of Murray and Simmonds (1991) that was adapted for Northern Hemisphere cyclones by Pinto et al. (2005). Cyclones are identified using the Laplacian of mean sea level pressure (MSLP) ($\nabla^2 p$), which is a proxy for the local geostrophic vorticity. The cyclone location is then identified as the minimum in MSLP that is closest to the maximum in $\nabla^2 p$, in order to relate the identified feature to a "real" low-pressure core. Tracks are filtered to remove weak (maximum $\nabla^2 \mathrm{p} > 0.6$ hPa deg.lat^{-2}), short-lived (cyclone lifetime $\geq$ 24 hours), and non-developing (maximum $\frac{d}{dt}\nabla^2 \mathrm{p} \geq 0.3$ hPa deg.lat^{-2} day^{-1}) cyclones based on the criteria from Pinto et al. (2009). This method has been shown to compare well to other tracking schemes in terms of individual tracks (Neu et al., 2013), and also for seasonal track statistics (Pinto et al., 2016), and has been used widely in the scientific literature (e.g. Raible et al., 2008; Flocas et al., 2010; Hofstätter et al., 2016). The track, genesis, and lysis density statistics are calculated on a seasonal basis following the method of Hoskins and Hodges (2002). Density statistics are calculated as the number density per month per 5° spherical cap. Track densities are calculated across the whole lifetime of all tracks, with genesis and lysis densities using the first and last time step of each track respectively.

In order to identify cyclogenesis on synoptic fronts, the fronts themselves must first be identified. To do this the method of Schemm and Sprenger (2015) and Schemm et al. (2015) is followed. This method identifies fronts as having a minimum gradient in equivalent potential temperature (θ_e) at 850 hPa of at least 3.5K per 100km. Furthermore, all fronts must have a minimum length of 500km. This ensures only synoptic scale features and not weak, baroclinic zones are identified. A further filter is applied to the data so that any frontal features within 2° latitude/longitude of another front are classified as the same feature. This method for identifying synoptic scale features has been tested and validated for all types of front in the Northern Hemisphere (Schemm and Sprenger, 2015; Schemm et al., 2015, 2018). There are other methods that can be used for frontal identification (i.e. Simmonds et al., 2012), and other choices of thermal parameter used in a method such as the one used in this study (e.g. θ, Thomas and Schultz (2019); θ_w, Berry et al. (2011)). In Schemm et al. (2018) it was shown that the use of θ, or θ_e produced consistent results, with θ_e being preferred due to its conservation for moist adiabatic motion, and use in operational frontal identifications

Hewson (1998).

2.1 | Classifying Secondary Cyclogenesis

To identify cyclogenesis on pre-existing fronts a similar method to that of Schemm et al. (2015) is used. The process described herein is also summarised in the decision tree in figure 1. In order to identify secondary cyclogenesis an objectively identified cyclone must first have its genesis point within 200km of a frontal feature. This front must also be connected to a pre-existing cyclone in order for the cyclone to be classed as secondary. The front is connected to another cyclone if it is located within 500km the cyclone. In situations when there are multiple cyclones within 500 km of a front which all satisfy the criteria to be a primary cyclone, only the closest cyclone to the front is taken as the primary cyclone. This ensures there is a one-to-one correspondence between primary cyclones and secondary cyclones. All cyclones that are classed as secondary or those that satisfy both the primary and secondary cyclone criteria (i.e. a secondary cyclone that later in its life is the primary cyclone to another secondary cyclone) are then classed as Secondary+ cyclones. This ensures that each cyclone family has one primary cyclone associated with it, but potentially multiple secondary cyclones. The first cyclone in a family is always classed as the Primary cyclone with any subsequent cyclones in a family being termed Secondary+ cyclones. Any cyclones that do not satisfy the criteria of being a Primary or a Secondary+ cyclone are classed as Solo cyclones. Solo cyclones may or may not be associated with fronts at some point in their lifecycle, if so, no cyclogenesis is occurring on any connected front.

Based on the above methodology three different types of cyclones are classified.

1. Primary: Cyclones associated with a frontal feature at some point during their lifetime, with the front subsequently being associated with the cyclogenesis of another cyclone. These are the first cyclones in a cyclone family.
2. Secondary+: Cyclones that form within 200km of a pre-existing front that are in turn associated with a previously identified cyclone. These cyclones are any that are not the first in a family.
3. Solo: These cyclones may be associated to fronts during their lifetime, but these fronts are not associated with cyclogenesis along them. Alternatively, they may have no associated frontal features at any point in their lifetime.

In parts of this study "Family" cyclones are also referred to. These cyclones are simply the sum of Primary and Secondary+ cyclones. For all of the classifications described in this section the methodology is applied to all cyclones in the northern hemisphere. In the results section of this study the focus will solely be on the North Atlantic and Western Europe and will present a subset of all the cyclone families identified. An illustrative example of the method is shown in figure 2. Sensitivity tests have shown that the number of Secondary+ cyclones identified is insensitive to the choice of search radius from the Primary cyclone. The number of Secondary+ cyclones identified is sensitive to the 200km cyclogenesis radii for cyclogenesis occurring along a front, however this radius was chosen to be most consistent with various objective case studies and similarity to previous work (Schemm and Sprenger, 2015; Schemm et al., 2018).

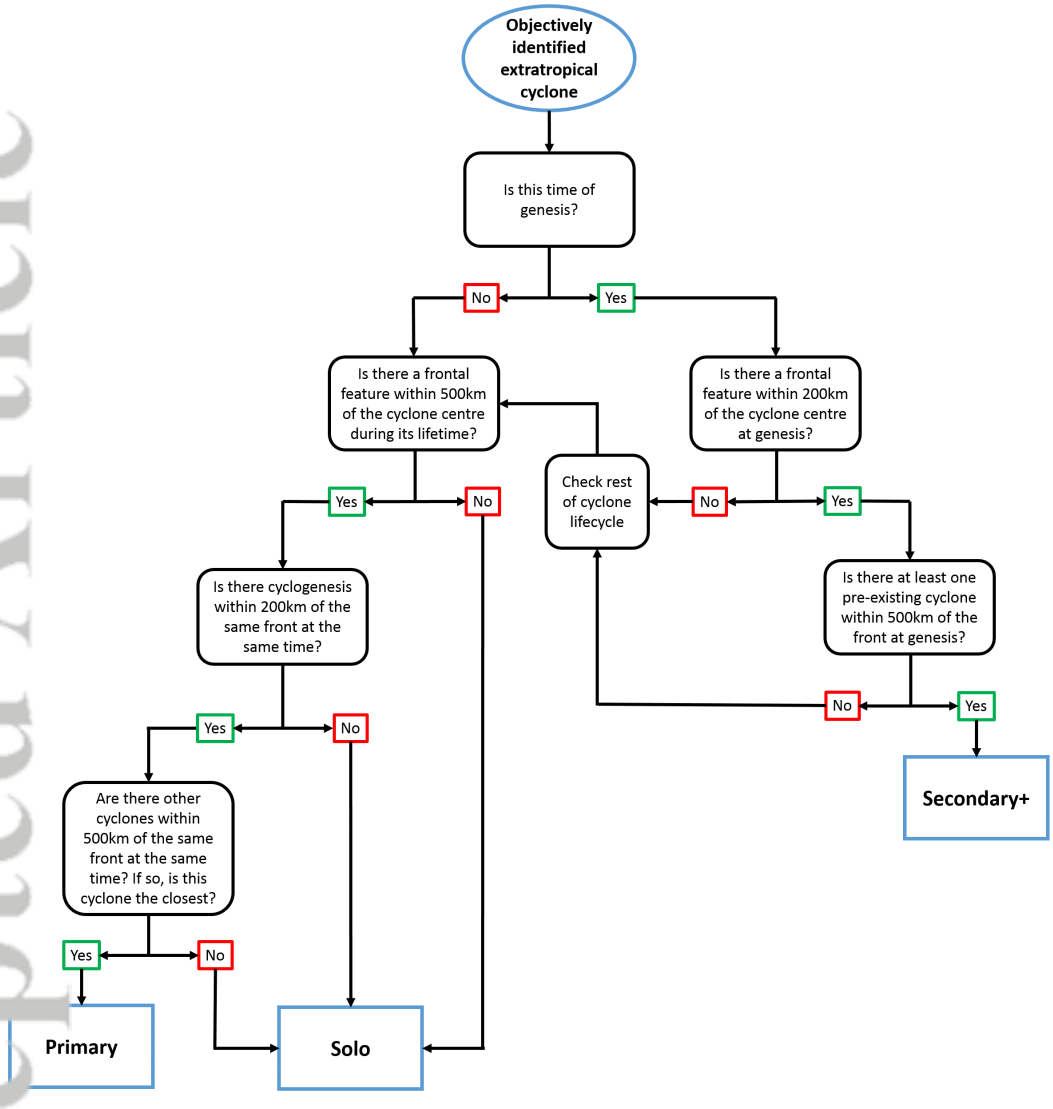

FIGURE 1 A decision tree for classifying the different types of cyclones that make up a cyclone family. Each cyclone can only be classified once.

4 | Large-scale Environmental Variables

To evaluate the state of the large-scale environment at times of Secondary+ cyclogenesis several variables are investigated. First of all the upper-level jet, which is taken as the 250 hPa wind speed anomaly from the 1979-2015 NDJFM climatology. Another upper-level feature investigated is that of the Rossby wave breaking (RWB). The method of Masato et al. (2013) is used to identify regions of RWB on the dynamical tropopause (2 potential vorticity unit (PVU) surface: 1 PVU = 1×10^{-6} K m^2 kg^{-1} s^{-1}). RWB is diagnosed as the reversal of the climatological meridional gradient

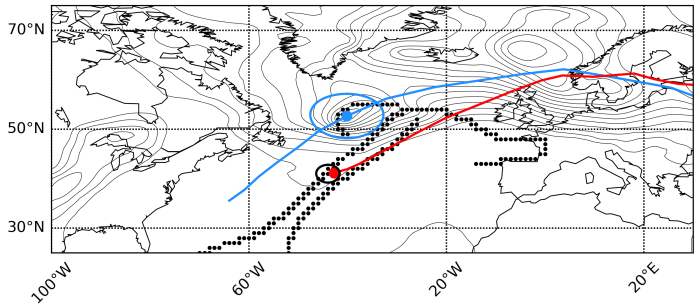

FIGURE 2 An illustrative example of how secondary cyclones and cyclone families are classified from 11th January 2007 at 1800. The blue line represents the entire cyclone track of a Primary cyclone, with the blue dot indicating the location at 1800 on 11/1/07. The red line is the entire cyclone track of the identified Secondary+ cyclone, with the red dot being its location at 1800 on 11/1/07. The blue circle is the 500km search radius for associating fronts to Primary cyclones. The black dots are the location of the connected front at 1800 on 11/1/07. The black circle indicates the 200km radius used to search for the cyclogenesis of a Secondary+ cyclone associated to the connected front. The light grey contours are mean sea level pressure.

in θ and will be expressed as an anomaly of the frequency of RWB in a particular location relative to the local climatological frequency (i.e. a frequency of 0.33 in a location where the climatology is 0.3 would have an anomaly value of 0.1, 0r 10%).

Furthermore, the environment of the lower atmosphere is investigated, specifically the low-level static stability (800-950 hPa averaged). The Brunt-Väisälä frequency (N^2) is calculated, which has been formulated in pressure (p) coordinates and it is expressed as a relative anomaly to the NDJFM climatology. The formulation for N^2 used is shown in equation 1 and is the local change of θ with pressure (p), that is also scaled by gravity (g), the mean layer temperature (T), and the specific gas constant (R).

$$N^2 = -\frac{pg^2}{RT\bar{\theta}}\frac{\partial\theta}{\partial p} \tag{1}$$

3 | RESULTS

3.1 | Climatology of Primary, Secondary+, and Solo Cyclones

Applying the identification criteria laid out in section 2.3 to 36 extended winters, an assessment of the properties of the different types of cyclones is performed. Figure 3a shows the total NDJFM track density of all cyclones and has a characteristic southwest-northeast tilt that extends from the eastern coast of North America toward the coast of Norway and the Nordic Seas. There is a maximum in the density of cyclone tracks in the region between the tip of Greenland and western Iceland, with values up to 20 cyclones per month. A further maxima in the track densities is identified across the central Mediterranean with a maxima of 10-13 cyclones per month downstream of the Gulf of Genoa.

The Primary cyclone class track density is shown in figure 3b. The mean spatial features of figure 3b are similar to that

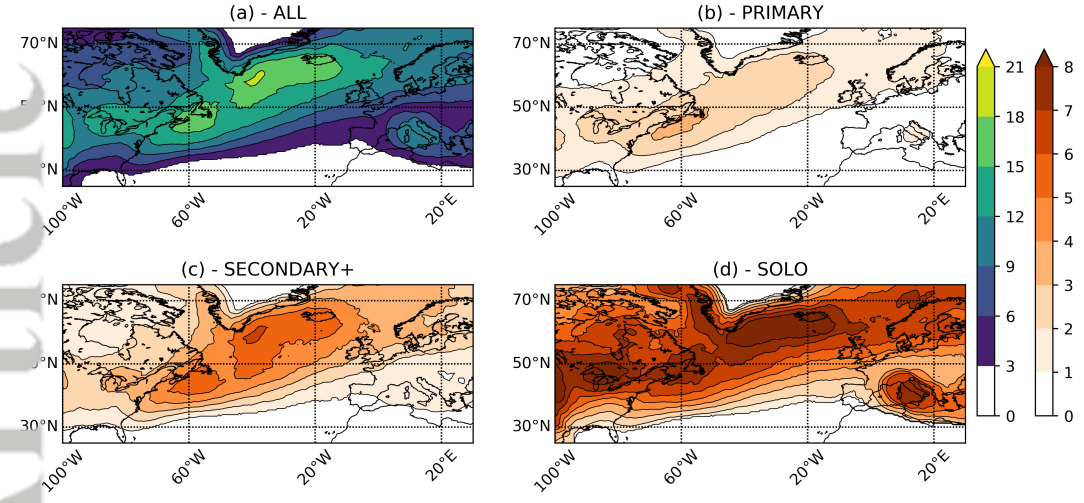

FIGURE 3 Track densities of (a) All cyclones, (b) Primary cyclones, (c) Secondary+ cyclones, and (d) Solo cyclones. Units of the densities are cyclones per month per 5° spherical cap. Lowest contour intervals are not coloured and regions less than 3 cyclones per month^{-1} per 5° spherical cap are masked out.

…igure 3a. For example, there is a characteristic SW-NE tilt in the North Atlantic, but the tracks are now concentrated closer to the east coast of North America, with values of approximately 3-4 cyclones per month in this region. P…mary cyclones do not travel as far to the NE as in figure 3a, with relatively lower track densities beyond 20°W.

…e track density of the Secondary+ cyclone class is shown in figure 3c. Again a SW-NE tilt is observed as in figure 3a and 3b. However, for Secondary+ cyclones the maxima in the track density covers a broader region of the North Atlantic (from approx. 40-10°W), with values of 5-7 cyclones per month. This suggests a difference in the …tial geographical location of Primary vs. Secondary+ cyclones in terms of the overall North Atlantic storm track. The Secondary+ cyclones may be further east than Primary cyclones due to Primary cyclones having to propa…e downstream somewhat before the genesis of the Secondary+ cyclones, as was observed by Schemm et al. (2018).

Th… final cyclone class is that of Solo cyclones (figure 3d). Solo cyclones exhibit different mean locations in track …ensity than the Primary and Secondary+ classes. Firstly, the characteristic SW-NE tilt of the track density is less pronounced. The largest densities are not confined to the ocean basin as for Primary and Secondary+ cyclones, with …latively large number of tracks present over the North American continent. The largest densities are in zonal band between the tip of Greenland and Iceland. The final dominant region for Solo cyclones is in the Mediterranean (>7 …clones per month), which is a large increase compared to the other classes.

Th… relative contribution of the different cyclone classes to the total track density is shown in figure 4. Primary cyclones are more prevalent in the western North Atlantic (figure 4a) and over the eastern coast of North America. They are dominant in the entrance region of the North Atlantic storm track where they make up 20-30% of all cyclones.

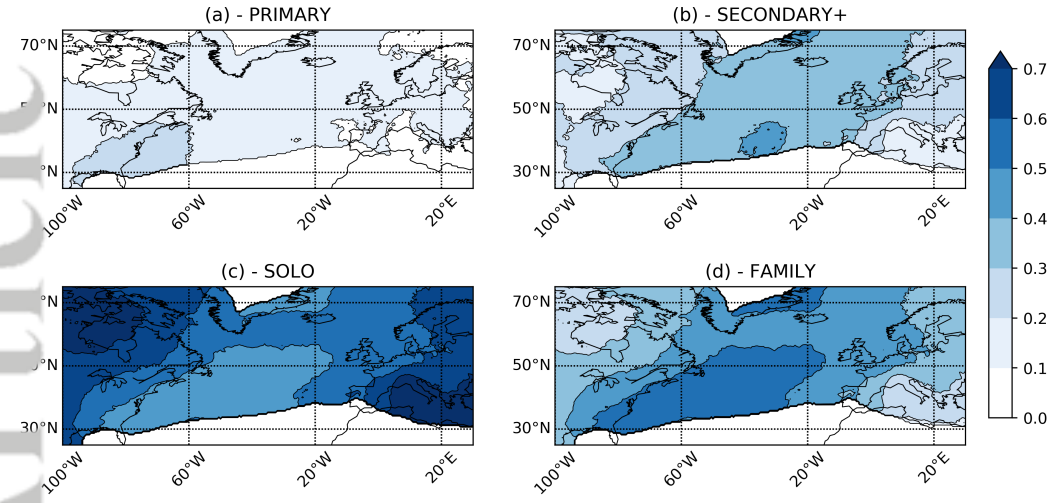

FIGURE 4 Fractional track density of each cyclone class compared to the overall track density for (a) Primary, (b) Secondary+, (c) Solo, and (d) Family (Primary + Secondary+) cyclones. Regions where the total track density is less than 3 cyclones per month are masked out in each figure.

Conversely, Secondary+ cyclones (figure 4b) have their largest contribution to the storm track across the central and eastern North Atlantic and extending NE toward the Nordic Seas. They make up 40-50% of all cyclones in the central North Atlantic and 30-40% of all cyclones across most of the rest of the North Atlantic basin and northwestern Europe. This pattern is somewhat similar to the findings from Schemm et al. (2018) (their figure 5b), however they found that cyclones forming on a trailing front made up 20-30% of all cyclones in the central/eastern North Atlantic. These differences are likely due to the differences in track densities between the cyclone identification method of Pinto et al. (2005) applied for this study, and the method of Wernli and Schwierz (2006) used by Schemm et al. (2018) in this region. Large differences in the track densities can be seen Pinto et al. (figure 2 of 2016), with up to twice as many cyclones per season in some parts of the equatorward central North Atlantic.

Grouping these two classes together results in the Family class (figure 4d). This illustrates how Family cyclones are most dominant in the main storm track region (figure 3a) and contribute up to 60% of all storm in the North Atlantic. The Family cyclones are strongly linked to the oceanic regions, with minimum values over continental regions, and are most prevalent across what one may consider to be the wintertime North Atlantic storm track.

Solo cyclones dominate different locations to Family cyclones. The relative contributions for Solo cyclones to the total density of cyclones (figure 4c) are North America, specifically northern Canada, and also the Mediterranean Sea. In both these regions Solo cyclones make up >70% of all cyclones. Solo cyclones are by definition the opposite of Family cyclones and are a smaller fraction of the total number of cyclone tracks across the North Atlantic (<50% of all cyclones across most of this region).

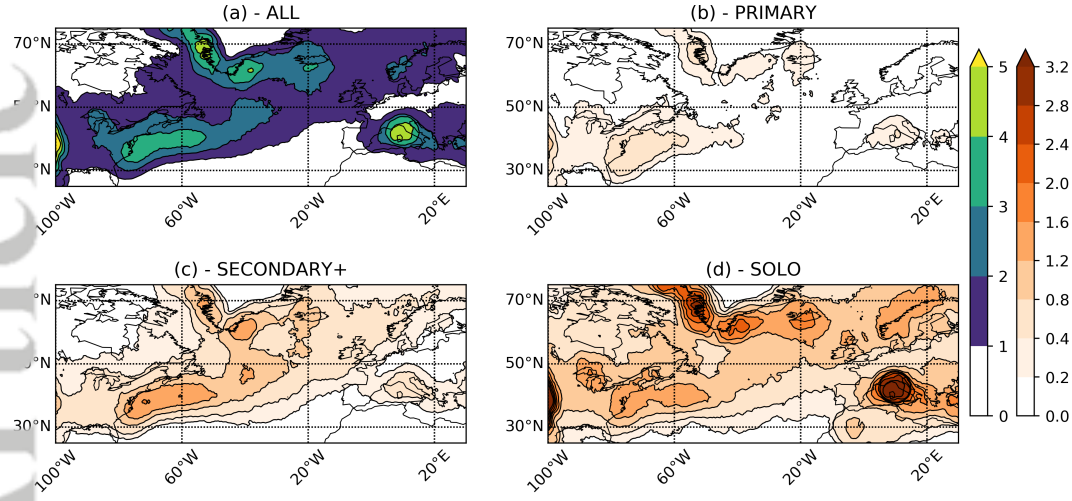

FIGURE 5 Genesis densities of (a) all cyclones, (b) Primary cyclones, (c) Secondary+ cyclones, and (d) Solo cyclones. Units of the densities are cyclones per month per 5° spherical cap. Lowest contour intervals are not coloured.

Further insight into the differences between the different classes of cyclone can be inferred from an examination of their genesis density climatologies (figure 5). One of the main genesis locations for all cyclones (figure 5a) is close to the eastern coast of North America and over the Gulf stream. This is to be expected as the quasi-permanent temperature gradient in this location generates baroclinic instability that is the dominant driver of mid-latitude cyclone formation. Other main regions for cyclogenesis are surrounding the tip of Greenland, over the Gulf of Genoa, and downstream of the Rocky Mountains.

For Primary cyclones (figure 5b), the dominant cyclogenesis region is over the Gulf stream. There are also Primary cyclones that form near the tip of Greenland and over the Mediterranean, but with fewer cyclones forming per month than over the Gulf stream. Unlike Primary cyclones, Secondary+ cyclones (figure 5c) have a tendency to form in the central North Atlantic. There is also a substantial amount of Secondary+ cyclogenesis near the coast of North America, which may be related to processes such as coastal frontogenesis (Bosart, 1975; Nielsen, 1989; Gyakum et al., 1996) or cold air damming. This difference in genesis density of Secondary+ and Primary cyclones, with Secondary+ cyclones tending to form further downstream can be understood as follows. Any Primary cyclone that forms over the Gulf stream then propagates in a SW-NE direction with the subsequent Secondary+ cyclone then forming on a trailing front, which is likely to be downstream of the Gulf stream.

The Solo cyclone class (figure 5d) has some cyclogenesis near the coast of North America and the western North Atlantic, however, unlike the other classes this is not the dominant region. The main regions are in the Mediterranean, the Lee of the Rocky mountains (not shown), and also surrounding the tip of Greenland. Given the mean location of

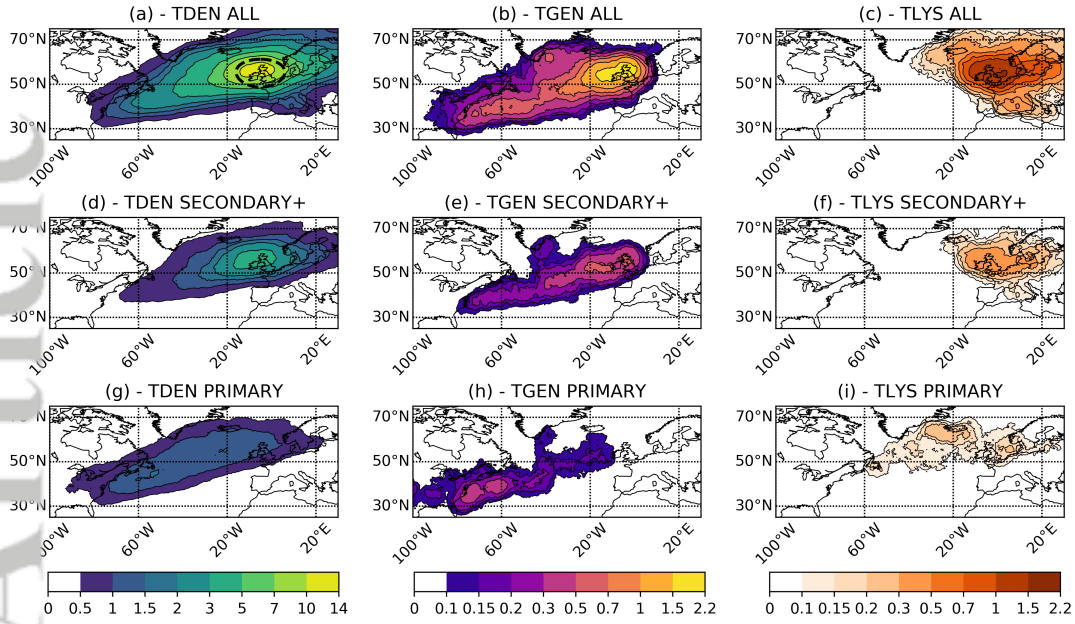

FIGURE 6 Density plots for all cyclones (a)-(c), Secondary+ cyclones (d)-(f), and the associated Primary cyclone of the Secondary+ cyclones (g)-(i) that pass through the 55°N region. (a,d,g) Track densities. (b,e,h) Genesis densities. (c,f,i) Lysis densities. The lowest contour intervals are not coloured. Units of the densities are cyclones per month per 5° spherical cap. The black dashed region in (a) represents the 700km region that cyclones must pass through.

Solo cyclogenesis it is possible that Solo cyclones are quite different from Family cyclones and could be more influenced by processes such as lee cyclogenesis.

The lysis densities of the different cyclone classes has also been investigated as part of this study. The lysis is shown in figure S1. The characteristics for the Primary and Secondary+ cyclone classes are very similar and both tend to their lysis in the region between Greenland and Iceland and more over the North Atlantic (this is consistent with the lysis for all cyclones; figure S1b/c). Solo cyclones tend to have their lysis across the Mediterranean, and also parts of North America and the region between Greenland and Iceland (figure S1d).

3.2 | Structure of a Cyclone Family

To examine the temporal and spatial relationships between Primary and Secondary+ cyclones, specific Secondary+ cyclone events are examined. To select these events only cyclones that track through a 700km radius centred at 55°N, 0°W are included (black dashed region in figure 6a). This area selection is consistent with Priestley et al. (2017b) and allows for a focus on cyclones that are affecting specific regions of western Europe.

For all storms that pass through the 55°N region, the track density (figure 6a) is of a more zonal orientation than the total storm track (figure 3a). Most cyclones are located between 50-60°N and east of 40°W. This is further ap-

parent when looking at the genesis of these cyclones (figure 6b) as most of the cyclones that pass through 55°N form very close to this region (east of 20°W). The average lysis of these cyclones (figure 6c) is to the east of the UK and mainly extending further east toward Denmark and across northern Europe. This suggests that a majority of cyclones tracking over the UK are short-lived features that form close to the European continent, propagate eastwards in a zonal direction before dissipating shortly afterwards (consistent with Dacre and Gray, 2009).

Similar density patterns are found when investigating the Secondary+ cyclones that pass through 55°N (figure 6d,e,f). These cyclones also form close to the UK and Europe (figure 6e), although, as in figure 6b, there are also cyclones that form over the western North Atlantic. The pattern of track density (figure 6d), is more zonal than the total track density for all storms (figure 3a) , before undergoing lysis to the east of the UK and over the North Sea and surrounding countries.

A different picture emerges when looking at the density pattern for the Primary cyclones that are in the same family and hence precede the Secondary+ cyclones analysed in figures 6d-f. Unlike the Secondary+ cyclones, which are constrained to pass through the 55°N region (figures 6d-f), the Primary cyclone of the family do not have this requirement. The average track density for these Primary cyclones (figure 6g) is different to those shown in figures 6d-f. The Primary cyclones exhibit the SW-NE tilt seen in figure 3b with a maximum in the density of cyclone tracks near the coast of North America, and also to the south of Iceland. It is interesting to note that the track density of Primary cyclones (figure 6g), and the genesis density of Secondary+ cyclones (figure 6e) exhibit a similar tilt with the Secondary+ genesis density being at a more southern latitude across the North Atlantic. A majority of the Primary cyclones have their genesis over the strong baroclinic zone off the east coast of North America (figure 6h), unlike the more downstream genesis locations of the Secondary+ cyclones. Finally, the lysis locations (figure 6i) for Primary cyclones is in the region between the tip of Greenland and Iceland. This suggests that these Primary cyclones do not travel near the European continent and are mainly constrained to longitudes west of 20°W. The similarity in the lysis longitude of the Primary cyclones (figure 6i) and the genesis of the Secondary+ cyclones (figure 6e) goes some way to confirm the hypothesis from Dacre and Gray (2009) that eastern North Atlantic cyclones are commonly Secondary+ cyclones.

In summary, the Primary cyclone tends to form over the Gulf stream and near the coast of North America before travelling in a NE direction across the North Atlantic. These cyclones then have their lysis to the east of Greenland, near Iceland. During their lifetime cyclogenesis occurs along an associated frontal feature, with this generally being located in the central to eastern North Atlantic and at a latitude of 50-60°N and to the south of the Primary cyclone. These Secondary+ cyclones then propagate in a much more zonal direction across the UK in this case before dissipating over the UK or the North Sea and its surrounding countries. This illustrates how these different cyclone classes tend to be preferentially located in different parts of the North Atlantic and also the North Atlantic storm track (as was suggested from figure 4). The results of figure 6 further highlights the misleading nature of mean track densities as noted by Whittaker and Horn (1984) due to the fact that cyclones rarely travel the length of the entire storm track and the mean storm track is made up of several different types of cyclone.

This analysis has also been performed for Secondary+ cyclones that pass through two other geographic regions for western Europe at 45°N, 5°W, and 65°N, 5°W, as defined in Priestley et al. (2017b), and their preceding Primary cyclones, which do not have to pass through the specified regions (see figure S2 and figure S3). The results of this was very similar to that presented in figure 6, with the main difference being northward/southward shift in the gen-

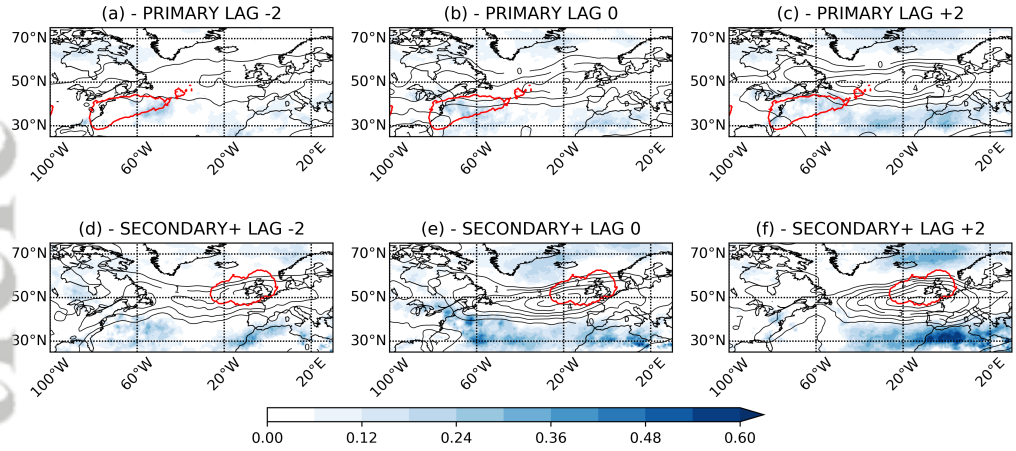

FIGURE 7 Composites of Rossby wave breaking (RWB) and the upper-level jet for Secondary+ cyclones that pass through the 55°N region and their respective Primary cyclones. Composites are at time of Primary cyclogenesis (b) and Secondary+ cyclogenesis (e). Also shown are composites at lag -2 days (a,d) and lag +2 days (c,f). Red contours in (a-c) are a contour of Primary cyclogenesis (at lag 0 days) that is 50% of the maximum value. Red contours in (d-f) are the same as (a-c) but for Secondary+ cyclones. RWB is expressed as an anomaly in the frequency of RWB at that location relative to the local climatological frequency and is shown by the blue shading. Each contour interval is a 6% increase in the frequency. The upper-level jet is illustrated by the black contours as an anomaly in the 250 hPa wind field to the local climatology in m s^{-1} with contours every 1 m s^{-1} above 1 m s^{-1} .

genesis/lysis latitude of the Secondary+ cyclones dependent on the latitude of interest. With this, there are only very minor shifts in the angle of the Primary cyclone mean track density. There are clear differences between the Primary cyclones and Secondary+ cyclones for all latitude subsets, with Primary cyclones having a more poleward component to their track than the Secondary+ cyclones that follow them. However, it is interesting to note that despite there being large differences in the latitude of Secondary+ cyclogenesis, the tracks of the Primary cyclones that precede them are so similar.

3.2 | Large-scale Environmental Conditions at the Time of Primary and Secondary+ Cyclogenesis

3.2.1 | Upper-level Jet and Rossby Wave Breaking

As illustrated in figure 6, the Secondary+ cyclones that pass through 55°N, and their respective Primary cyclones, form in different locations and are also likely to form under different environmental conditions. To understand any differences, the upper-level features that are associated with these cyclones at their time of genesis is analysed (figure 7). As has been established in several studies, cyclones that impact western Europe are commonly associated with an anomalously strong upper-level jet and RWB on one or both sides of the jet (Hanley and Caballero, 2012; Gõmara et al., 2014; Pinto et al., 2014; Messori and Caballero, 2015; Priestley et al., 2017b), and therefore the same fields will be analysed herein.

The first focus is the time of cyclogenesis for Secondary+ cyclones passing through our 55°N region (figure 7e), and the cyclogenesis time of their respective Primary cyclones (figure 7b). These will be referred to as lag 0 days. Firstly, for the Primary cyclones (figure 7b), it is seen that anomalies in the upper-level jet and RWB frequency are very small. Jet anomalies are less than 3 m s^{-1}, with RWB frequency anomalies generally less than 10%, with some localised regions being ~20% above the climatological frequency. The cyclones are mostly all forming off the east coast of North America, near the right entrance of the jet, and the environment at this time can be mostly described as climatological, with minor positive anomalies.

At the time of Secondary+ cyclone genesis (figure 7e) the upper-level environment is very different. There are anomalies in the upper-level jet of over 5 m s^{-1} and anomalous RWB frequencies of up to 40% above the climatological frequency. Both fields have increased anomalies compared to the time of cyclogenesis of the Primary cyclones. This environment is representative of what was described in the aforementioned studies (Pinto et al., 2014; Priestley et al., 2017b), with anomalous RWB either side of an zonally extended and strong jet being favourable for the formation and presence of intense cyclones in the eastern North Atlantic. At the time of cyclogenesis, the Secondary+ cyclones are forming either on the jet axis or the left exit region of the jet, this suggests that conditions are favourable for cyclogenesis via upper-level divergence provided by the ageostrophic circulations in the left exit region of the jet (Rivière and Joly, 2006a,b).

Through inspection of the lag plots, further insight is gained into the connection between the Primary and Secondary+ cyclones. At lag 2 days after Primary cyclone formation (figure 7c) there is an amplification of the anomalies from lag 0 (figure 7b) downstream of cyclogenesis and around Iceland and the Nordic Seas. These anomalies are associated with the presence of the Primary cyclone in this region as it is likely to have propagated toward the NE from its genesis region. The presence of the Primary cyclone is associated with the development of anomalous RWB, which then in turn causes an acceleration in the jet (see figure 3 Priestley et al., 2017b) through the convergence of eddy momentum (Barnes and Hartmann, 2012). The state of the environment in figure 7c, is similar to that at Secondary+ cyclogenesis time (figure 7e), albeit with slightly reduced RWB anomalies, suggesting that the Primary cyclone might be key in creating an upper-level environment that is favourable for the formation of Secondary+ cyclones. Further evidence for this is provided in figure 7d. 2 days prior to Secondary+ cyclogenesis the upper-level environment has very small anomalies in RWB and the jet, which is very similar to figure 7b, and anomalies are almost zero 2 days prior to Primary cyclogenesis (figure 7a), suggesting that the anomalies are associated with the development and propagation of the Primary cyclone in the days prior to Secondary+ cyclogenesis. Anomalies are then amplified to an even greater extent as the Secondary+ cyclone develops and moves downstream (figure 7f), with anomalies of RWB more than 60% above the climatology and a very anomalous jet at 250 hPa (> 6 m s^{-1}).

As with figure 6, this analysis of figure 7 is repeated for Secondary+ cyclones passing through two other geographic regions at 45°N and 65°N, and their preceding Primary cyclones (figures S4 and S5). Similar results as those presented in figure 7 are found, yet with a different balance of the RWB to being more dominant on either the northern or southern flank, and hence a shift in the latitude of the jet anomalies, for cyclones impacting 45°N (figure S4) and 65°N (figure S5) respectively, as seen in Priestley et al. (2017b). These differences in RWB and Primary cyclone genesis/lysis could be interpreted through the two different baroclinic lifecycles (LC1/LC2) as first discussed by Thorncroft et al. (1993). Primary cyclones that spawn the 65°N Secondary+ cyclones may be more like the LC1 lifecycle. The Primary cyclone appears to form under more anticyclonic shear (figure S5b). LC1 cyclones are associated with anticyclonic RWB on the equatorward flank of the jet and a northward displacement of the jet, which is similar to what is seen in figure

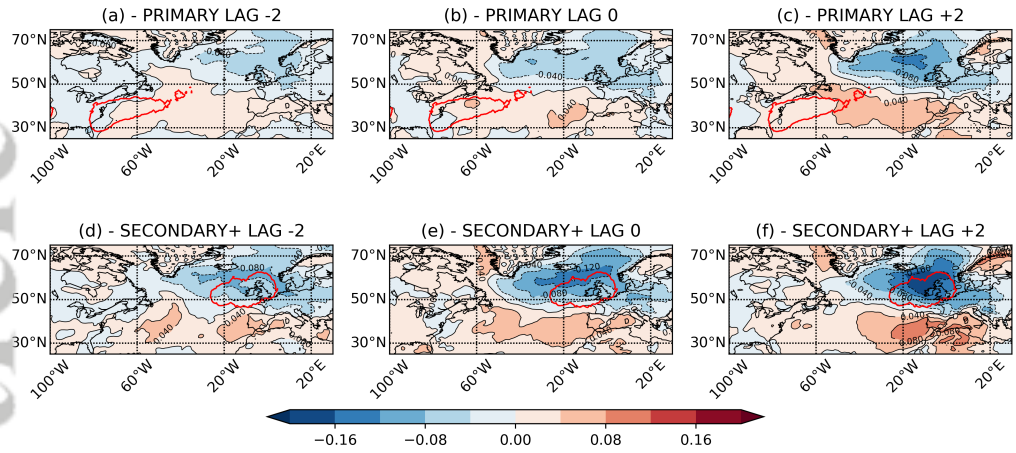

FIGURE 8 Composites of low-level static stability (N^2) for Secondary+ cyclones that pass through the 55°N region and their respective Primary cyclones are shown by the coloured shading. Composites are at time of Primary cyclogenesis (b) and Secondary+ cyclogenesis (e). Also shown are composites at lag -2 days (a,d) and lag +2 days (c,f). Red contours in (a-c) are a contour of Primary cyclogenesis (at lag 0 days) that is 50% of the maximum value. Red contours in (d-f) are the same as (a-c) but for Secondary+ cyclones. Anomalies are expressed as percentage changes relative to the local climatology.

The lysis of these 65°N Primary cyclones (see figure 9a) also occurs close to the jet axis, with part of the lifecycle even being on the equatorward side of the anomalous jet, further suggesting this could be propagating under the LC1 lifecycle. Conversely, the 45°N Primary cyclones appear to form under relatively neutral/cyclonic shear (figure S4b). The LC2 lifecycle results in a large amount of cyclonic RWB and a southward displacement of the jet, as is suggested (figure S4. The lysis of the 45°N cyclones also occurs quite far from the jet axis (figure 9c), indicating these Primary cyclones may be more like the LC2 lifecycle. These results suggest that the environment surrounding the Primary cyclone at the time of genesis is associated with differing lifecycles and RWB structures downstream, therefore affecting the latitude of Secondary+ cyclogenesis and latitude of propagation into western Europe.

3.3.2 | Low-level Static Stability

As cyclones forming in eastern North Atlantic are associated with a low stability environment (Dacre and Gray, 2009; Wang and Rogers, 2001), and that Secondary+ cyclones are also associated with reduced low-level stability anomalies (Schemm et al., 2015), the evolution of the low-level stability field at the time of Secondary+ cyclogenesis is investigated. Their respective Primary cyclones will also be analysed.

At the time of cyclogenesis (lag 0 days) for the Primary cyclone (figure 8b) there are minimal anomalies (<5%) in static stability across the North Atlantic, with some indication of a N-S dipole between 0-20°W, across 50°N. In the region of Primary cyclone formation anomalies are very weak and do not exceed ±4%. This process is likely to not be influenced by the stability as it is common for cyclones forming in this region to be Type B cyclones (Gray and Dacre, 2006) that are driven by an upper-level feature interacting with the quasi-persistent temperature gradients (Petterssen et al., 1955; Davis and Emanuel, 1991).

Conversely, at the time of Secondary+ cyclone formation (figure 8e), the dipole in anomalous N^2 is much larger, with anomalies more than 12% lower than the local climatology in the northeastern North Atlantic, and on average more negative than the anomalies in the region of Primary cyclogenesis. It is in this region of lower N^2 that the Secondary+ cyclones are forming. Cyclogenesis in low N^2 environments of the eastern North Atlantic has been previously studied (Lang and Rogers, 2001; Dacre and Gray, 2009), however it is interesting the note that as in figure 7, the negative anomalies in N^2 are much stronger at the time of Secondary+ cyclogenesis, compared to Primary cyclogenesis. As the Secondary+ cyclones are forming in a strongly anomalous low N^2 region, it appears that this low stability is important for Secondary+ cyclones to form.

As in figure 7, an amplification of the anomalies associated with the Primary cyclones from lag 0 days to lag 2 days is seen (figure 8b,c), and an increase in the anomalies from lag -2 days to lag 0 days for Secondary+ cyclogenesis (figure 8d,e). This increase in the anomaly magnitude is again likely associated with the propagation of the Primary cyclone downstream and in a northeasterly direction over a period of approximately 2 days. This amplification of the anomalies in N^2 can be understood through interpreting the thermal wind balance equation. The acceleration of the jet shown in figure 7 will have an increasing magnitude with height from the surface to the tropopause. Through thermal wind balance there will be an associated increase in the meridional temperature gradient near the surface at the time of Secondary+ cyclogenesis (not shown). This increase in the meridional temperature gradient below the jet axis is expected due to the Secondary+ cyclones forming along a nearby frontal feature. With the increase in meridional temperature gradient there will also be an increase of the vertical potential temperature gradient. This will be associated with an increase in the meridional gradient of static stability. Therefore as the Primary cyclone propagates NE, it is associated with an increase in RWB and hence an acceleration of the jet. This jet speed increase is then associated with an enhanced temperature gradient across the jet axis and a stronger stability dipole. This results in a stability minima at low-levels on the northern flank of the jet. This anomalously low stability environment is then helpful for the formation and intensification of Secondary+ cyclones in this region. This environmental development is associated with the downstream propagation, development, and presence of the Primary cyclone in the 2-3 days prior to the Secondary+ cyclogenesis. A further explanation of this process is given in Appendix A.

As with figures 6 and 7, this analysis was repeated for Secondary+ cyclones passing through our regions at 45°N and 65°N, and their preceding Primary cyclones (figures S6 and S7). Similar results are found with the dipole in stability anomalies closely following the jet axis and moving south or north for Secondary+ cyclones impacting 45°N (figure S6) and 65°N (figure S7) respectively. The role of the jet anomalies in driving the latitude of the stability anomalies is clear, with the evolution of the anomalies with the downstream propagation of the Primary cyclone also being further apparent.

The relationships identified in sections 3.2 and 3.3 are brought together, illustrated, and summarised in figure 9. It is shown in figure 9 how for Secondary+ cyclones passing through the different geographical regions (65°, 55°, 45°N) the Secondary+ cyclones form close to the European continent, with their preceding Primary cyclones forming over the Gulf stream and near the coast of North America and having their lysis over the central North Atlantic. The occurrence of RWB on one or both sides of the jet affects the tilt of the jet in the exit region and is could be a result of different baroclinic lifecycles of the Primary cyclones. The acceleration of the jet is then associated with an amplification of the stability dipole in a north-south direction across the jet, which likely further aids the cyclogenesis and intensification progress of Secondary+ cyclones. Variations in these anomalies are then associated with changes

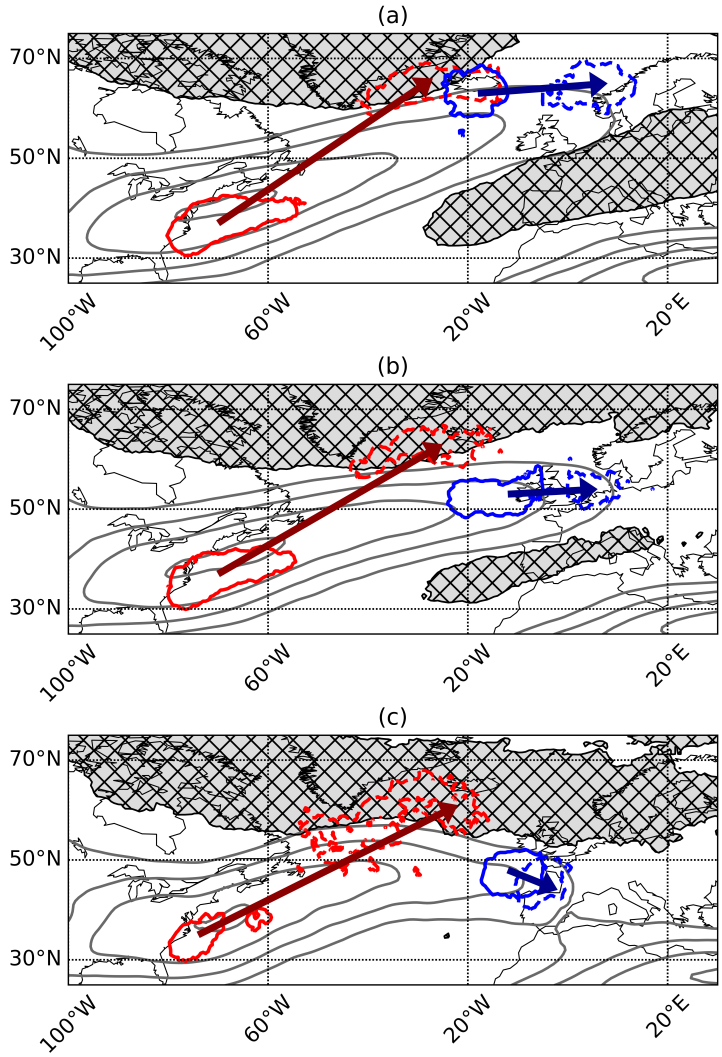

FIGURE 9 A summary figure illustrating the genesis (solid contours) and lysis (dashed contours) of Primary cyclones (red) and their subsequent Secondary+ cyclones (blue) that pass through the (a) 65°N region, (b) 55°N region, and (c) 45°N region. Also shown are contours of the 250 hPa wind speed (grey contours, every 5 m s^{-1} above 30 m s^{-1}) and regions of RWB (grey hatching) averaged throughout the lifetime of the Secondary+ cyclones.

the genesis latitude and subsequent track of the Secondary+ cyclones toward western Europe.

3.4 | Secondary+ cyclones and clustering over western Europe

In this section of the paper the importance of Secondary+ cyclones for periods of clustering is investigated. The aim is to understand the relative roles of Secondary+ cyclogenesis and steering by the large-scale flow on the increase

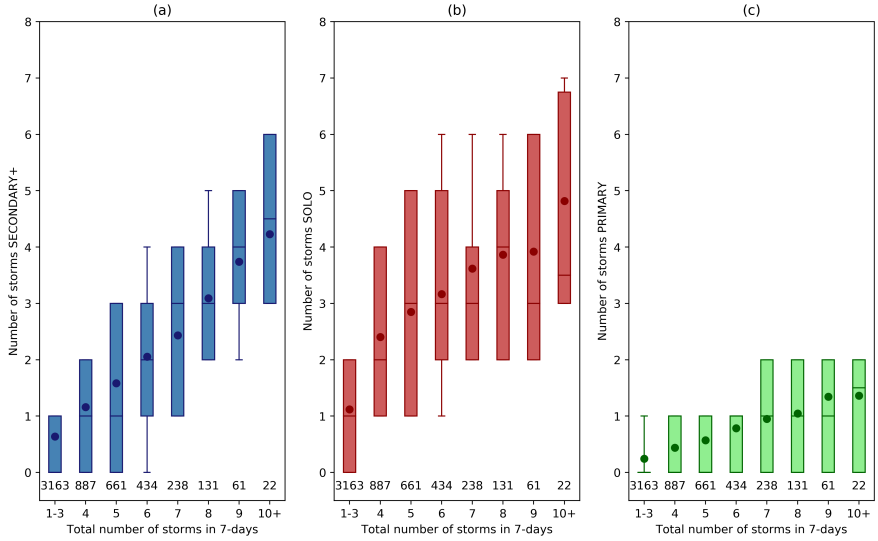

FIGURE 10 Number of Secondary+ (a), Solo (b), and Primary (c) cyclones compared to the total number of cyclones passing through the 55°N region in a period of 7-days. Boxes show the inter-quartile range, with the lines in the boxes representing the median and the dots being the mean. Whiskers extend to the 20th and 80th percentiles. Numbers below each box represent the number of data points in that bin.

in the number of cyclones during these periods. Following Pinto et al. (2014); Priestley et al. (2017b), clustering is defined to be more than 4 cyclones in a 7 day period for cyclones that pass through the 55°N region. The results of this are shown in figure 10.

For all of the cyclone classes shown in figure 10 there is an increase in the number of cyclones in each class as cyclones pass through the 700km 55°N region more frequently. However, the rate of increase is different for each of the classes. Firstly, the number of Secondary+ cyclones (figure 10a) increases almost linearly from less than 1 cyclone in 7-days for non-clustered periods, to an average of 4 cyclones in 7-days during the most intensely clustered periods. A similar relationship is seen for Solo cyclones (figure 10b). There is ~1 Solo cyclone in 7-days in non-clustered periods, with a mean of ~5 in 7-days for the most clustered events. A different relationship is found for Primary cyclones (figure 10c). There is still an increase in the mean number of Primary cyclones as the intensity of clustering increases, yet the total number is much lower. There are at most 2 Primary cyclones in 7-days, with the average during non-clustered periods being ~0.2 cyclones per 7-days, and an average of ~1.5 cyclones in 7-days during the most clustered periods. This lower number of Primary cyclones is what would be expected from figures 3b and 6g as it is shown that Primary cyclones rarely have a presence over western and north-western Europe, with this especially being the case for the 55°N cyclone families.

On average Secondary+ cyclones make up ~50% of cyclones during severely clustered periods when more than 10 cyclones are passing through the 55°N region in one week. From figure 10 it is also interesting to note the difference

in the increase in the Secondary+ and Solo cyclones with the intensity of clustering, compared to the lesser absolute increase in Primary cyclones. This could be due to an increase in cyclogenesis near the UK of Secondary+ cyclones that would be assisted by the reduced stability environment associated with the development and propagation of the prior Primary cyclone (figure 8). This would result in more Secondary+ cyclogenesis occurring and an increased contribution from cyclone families as the intensity of clustering increases. Alternatively, the amount of cyclogenesis may not be increasing, and the large-scale flow (figure 7) may be much more dominant in steering all the cyclones along a similar track. This would lead to a large increase in the number of Secondary+ cyclones with a minimal increase in the number of Primary cyclones as these rarely interact with western Europe.

To understand if the dominant influence is an increase in cyclogenesis or the result of large-scale steering the Secondary+ cyclones that form in the North Atlantic during clustering periods (including 3 days prior to allow for propagation across the UK), and those during non-clustered periods are inspected. The results are shown in figure 11. Genesis densities of all Secondary+ cyclones that form during clustered periods are shown in figure 11a with the anomaly to non-clustered periods being shown in figure 11c. During periods of clustering there is an increase in cyclogenesis over the UK and slightly to the west, with decreases around the seas surrounding Greenland and Iceland, and also a decrease in the central North Atlantic. Both of these negative anomalies are regions that are commonly associated with Secondary+ cyclogenesis (figure 5c). It is also of interest to note that the relative number of cyclones forming per day across the entire North Atlantic basin is higher for non-clustered days compared to clustered days.

There are also changes in Secondary+ track density (figure 11b/d) with an increase in the number of tracks over the UK by more than three cyclones per month. As with the cyclogenesis, there is also a decrease in track density in the region surrounding Greenland and Iceland. This shift south seen in the cyclogenesis density and track density (figures 11c/d) is likely a result of the double-sided pattern of RWB associated with Secondary+ cyclone propagation into the UK (figure 7f) and also the same pattern associated with periods of clustering (Priestley et al., 2017b). This double-sided RWB pattern concentrates the formation of the Secondary+ cyclones further south than normal and over the region of low static stability (figure 8f). The jet anomaly between the regions of RWB forces all cyclones to follow a similar track toward western Europe, as is seen in figure 11.

Changes in Primary cyclogenesis and track density are shown in figure 11e/f. Over the main cyclogenesis region of the Gulf stream there are small changes in the rate of genesis of Primary cyclogenesis during periods of clustering (figure 11e), which would be expected as these cyclones generally form through baroclinic instability near the coast of North America. Cyclogenesis rate changes in the western North Atlantic do not exceed ±0.5 cyclones per month and rarely exceed ±0.15 cyclones per month for these Primary cyclones. There are very small increases in the rate of Primary cyclogenesis over the eastern North Atlantic and the UK, however these are locally very small. There are pronounced differences in the track density of the Primary cyclones (figure 11f) with an extension and zonalisation of the tracks over the UK leading to an increase of 1.5 cyclones per month. This anomaly is likely due to the enhanced upper-level flow associated with periods of clustering (Pinto et al., 2014; Priestley et al., 2017b) causing a more eastward propagation of the cyclones. This eastward propagation of the Primary cyclones also helps explain the negative anomalies in Secondary+ cyclogenesis in the central North Atlantic (figure 11c). As the Primary cyclones are likely travelling downstream at a faster rate, the Secondary+ cyclogenesis will be occurring further east than what would normally be expected, resulting in a negative anomaly in the main cyclogenesis region, as is seen in figure 11c. Consistent with this is that approximately 70% of the changes in the track density over the UK in figure 11b/d is a result of the cyclones that form east of 40°W (not shown).

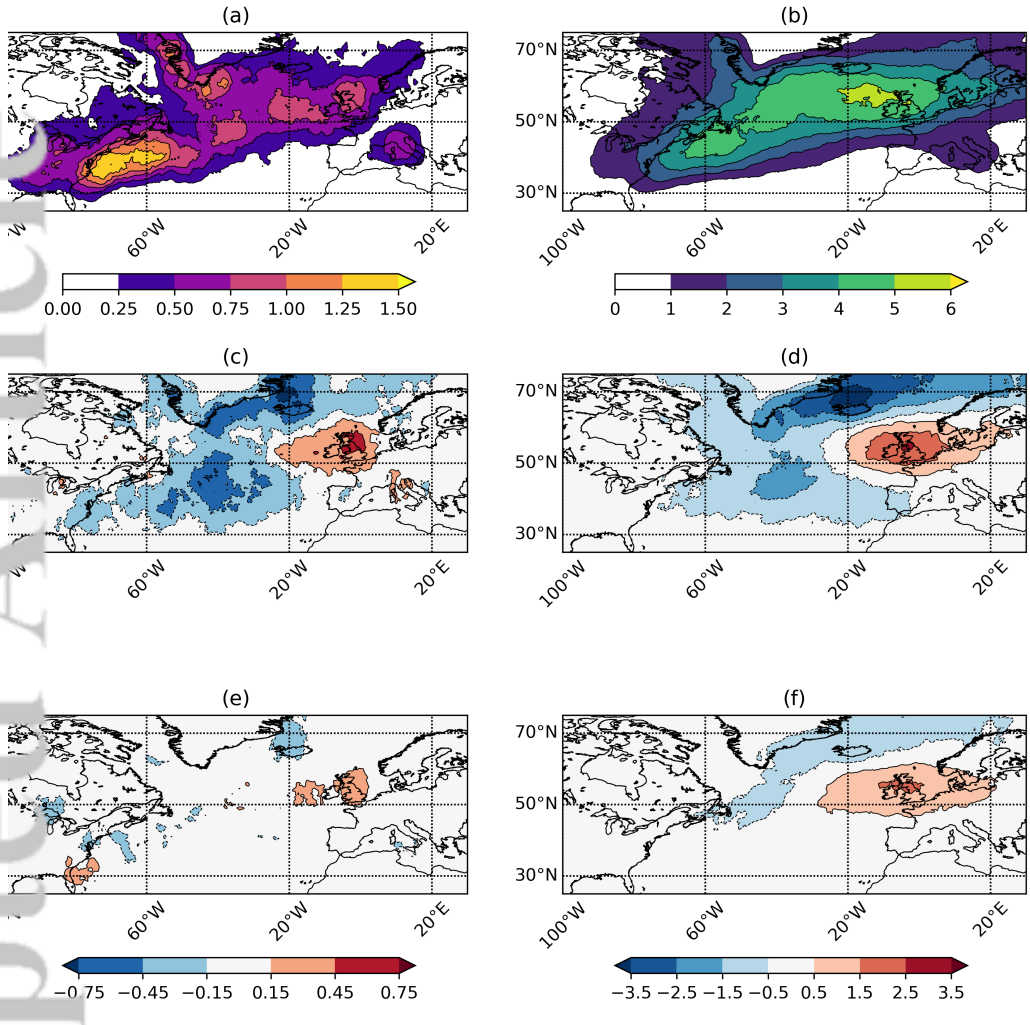

FIGURE 11 Genesis densities of Secondary+ cyclones during clustered periods (a) and their respective track densities (b). Anomalies of (a) and (b) relative to non-clustered periods are shown in (c) and (d) respectively. The anomalies of Primary cyclogenesis density and track density in clustered periods relative to non-clustered periods are shown in (e) and (f). In all panels units are number of cyclones per 5 degree spherical cap per month.

Furthermore, there are similar changes in the genesis rates and track densities of Solo cyclones (not shown) during clustered periods compared to non-clustered periods as with Secondary+ cyclones, albeit with less of a negative anomaly over the central North Atlantic as this is not a common region for Solo cyclogenesis.

Therefore, this analysis shows that as clustering becomes more intense, the number of Secondary+ cyclones becomes larger, with approximately 50% of cyclones being Secondary+ cyclones during extreme periods of clustering. While

there is an overall increase in the amount of Secondary+ cyclogenesis near to the UK, there is actually a basin-wide reduction in the cyclogenesis rate and less overall cyclones present (relative number per day) in the North Atlantic. Therefore indicating that the large-scale environment redistributes secondary cyclones during periods of clustering rather than increasing the total number of secondary cyclones. The difference during clustered periods is those that do develop are forming preferentially close to western Europe with this increase in the number of cyclones appearing to be driven by the dominant steering from the RWB and jet anomalies associated with this. This steering acts to concentrate all Secondary+ cyclones that form to travel along a similar track, with changes in the frequency of the RWB to the north and south of the jet affecting the jet angle and hence the genesis latitude and impact latitude of the Secondary+ cyclones. In Walz et al. (2018) the variability of clustering near the UK was shown to be associated with the different phases of the NAO and EA patterns, and the double-sided pattern of the RWB in figure 7e-7f has been shown to project onto the NAO (Messori and Caballero, 2015). Therefore, large-scale patterns such as the NAO/EA may play a role in modulating the occurrence of Secondary+ cyclones across the UK and other parts of western Europe.

4 | SUMMARY AND DISCUSSION

In this study the occurrence of Secondary+ cyclones and the cyclone families which they are a part of, and how these phenomena contribute to the North Atlantic storm track are investigated. Despite the comprehensive analysis of secondary cyclones by Schemm and Sprenger (2015) and Schemm et al. (2018) they did not objectively identify and compare the related primary cyclones, or quantify any differences in their preferential locations of genesis, track, and lysis. To identify Secondary+ cyclones and their associated Primary cyclones the method of Schemm and Sprenger (2015) is followed and applied to the cyclone identification and tracking algorithm of Murray and Simmonds (1991). Three distinctly different cyclone classes are identified, these are: Primary, Secondary+, and Solo. The main results of this study are as follows:

- Primary and Secondary+ cyclone classes make up more than 50% of all cyclones across the North Atlantic ocean, therefore they are vital for the structure of the North Atlantic storm track. Primary cyclones tend to form over the Gulf stream and are commonly found close to the coast of North America and the western North Atlantic ocean. Secondary+ cyclones form over the Gulf stream, but also the central North Atlantic. Solo cyclones are most commonly found over continents, the Mediterranean, and the high latitude North Atlantic. The preferential locations of the Secondary+ cyclones across the central and eastern North Atlantic is a result of Primary cyclones propagating in a northeasterly direction from where they form near the Gulf stream with Secondary+ cyclones then most likely forming on their southern flank.
- Primary cyclones are associated with the development of an environment that is favourable for Secondary+ cyclone formation and downstream propagation toward Europe. The Primary cyclone development is associated with an increase in RWB on one or both flanks of the jet, which is generally zonally extended and strengthened toward Europe. The enhanced jet is associated with a reduction in low-level static stability on the poleward flank of the jet, hence making the environment surrounding Secondary+ cyclogenesis more favourable for cyclone formation and development around the left exit region of the jet.
- Secondary+ cyclones contribute approximately 50% of cyclones during clustered periods. There is also an increase in the number of Solo cyclones, with a smaller increase in the number of Primary cyclones. The increase in the number of Secondary+ cyclones during clustered periods is mainly a result of the influence of the large-scale flow

steering all cyclones along a similarly zonal path toward western Europe and not an overall increase in cyclogenesis. The presence of the RWB acts to shift the main region of cyclogenesis further south to be at the same latitude as the region impacted by the clustering.

As Primary and Secondary+ cyclones are most commonly found over the western and central/eastern sectors of the North Atlantic, it is clear they are important for the overall structure of the North Atlantic storm track. The spatial separation of the two classes also illustrates the findings of Whittaker and Horn (1984) that individual cyclones rarely travel the entire length of the North Atlantic storm track, with those impacting Europe commonly forming very close to the continent (see also Hoskins and Hodges, 2002; Wernli and Schwierz, 2006; Dacre and Gray, 2009). The relative contributions of Secondary+ cyclones in the central North Atlantic are higher in this study than that found by Schemm et al. (2018). These differences likely arise from the differences in the cyclone identification and tracking schemes applied, with the Wernli and Schwierz (2006) method used in the aforementioned study commonly identifying only half as many cyclones as the Murray and Simmonds (1991) scheme used in this study (see figure 2 in Pinto et al., 2016). Furthermore as the overall number of cyclones identified by the Wernli and Schwierz (2006) scheme is lower than the Murray and Simmonds (1991) scheme used in this study, it may be that the fractional number of cyclones contributing to periods of clustering is still consistent amongst the methods. This would prove an interesting area of further exploration.

Primary and Secondary+ cyclones follow different track orientations with Primary cyclones propagating more poleward and Secondary+ cyclones having a more zonal nature to their track. For Secondary+ cyclones impacting western Europe their latitude of genesis is modulated by the presence of an anomalously strong jet and RWB and the Secondary+ cyclones are generally forming in the left exit region of the extended upper-level jet. These jet and RWB anomalies amplify with the downstream propagation of the preceding Primary cyclones. It might be possible that the differences in the jet/RWB response to the Primary cyclone are a result of differing baroclinic lifecycles of Primary cyclones (Thorncroft et al., 1993) and the differing momentum fluxes associated with the wave breaking from the two lifecycles. Based upon the jet/RWB pattern that is generated with the passage of these cyclones families into Europe it could be hypothesised that the passages of these families in specific locations are associated with various phases of the NAO or EA (see Messori and Caballero, 2015; Walz et al., 2018), with the Primary cyclones potentially playing a key role in modulating these large-scale patterns of variability on daily timescales (Rivière and Orlanski, 2007; Gõmara et al., 2014).

Secondary+ cyclones are also shown to form in regions of reduced low-level static stability, with the region of low stability being dictated by the latitude of the jet exit. These findings aligns with Schemm and Sprenger (2015), and also Wang and Rogers (2001) and Dacre and Gray (2009) who illustrated that cyclones forming in the eastern North Atlantic were more commonly associated with a lower stability environment. It is likely that the reduced stability is contributing to the faster growth or deeper cyclones and not additional genesis (Dacre and Gray, 2006). These results, coupled with the common genesis of cyclones in the eastern North Atlantic adds further evidence to the hypothesis from Dacre and Gray (2009) that Secondary+ cyclones are most closely aligned with Type C cyclogenesis. The cyclogenesis locations also suggest that our Primary cyclones may be closely aligned with Type B cyclones, and Solo cyclones to Type A cyclones. These classifications and their relationships to the cyclone families is something that could be quantified further using a quasi-geostrophic vertical velocity framework to distinguish the cyclone types (as in; Deveson et al., 2002; Plant et al., 2003).

There are several limitations to this study. Firstly, only one re-analysis product was utilised (ERA-Interim), and only 36 years of data from it. Future avenues of research could include investigating secondary cyclones in other re-analysis products, with the results from this study compared using consistent time periods from multiple products. In addition, just one cyclone identification and tracking algorithm has been used, and one method to identify synoptic-scale frontal features. Results have been shown to be sensitive to the choice of cyclone identification methodology, although most methods are consistent for mature phases of the cyclones lifecycle, particularly for intense systems (Neu et al., 2013). However, it would be of interest to compare the results of this study, and those of Schemm and Sprenger (2015), with results from other identification schemes. Other frontal identification schemes are also available (e.g. Hewson, 1998; Simmonds et al., 2012), and it would be of interest to compare our results to results from Secondary+ cyclones identified using a different methodology.

Further directions for research could also include an investigation into the process of frontal-wave cyclogenesis for other oceanic basins such as the Pacific, as this process also occurs in other geographic regions (Schemm et al., 2018). In addition, a quantification of the role of the NAO, or other leading atmospheric patterns in controlling the density of Secondary+ cyclones would be of interest. Furthermore, with the database of cyclone types that has been created in this study, examination into the physical differences (e.g. lifecycle, intensity, deepening rate, structure, etc.) of the different classes would be of interest. Previous studies have shown differences in eastern and western North Atlantic cyclones and their evolution characteristics (e.g. Dacre and Gray, 2009; Čampa and Wernli, 2012), with the assumption that the two regional cyclones are systematically different, and performing the same analysis for Primary versus Secondary+ cyclones would be an interesting addition to this analysis.

With regards to the results presented in this study, further in-depth analysis of the processes driving our Secondary+ cyclones would be of interest, especially to build on the results of Schemm and Sprenger (2015) and investigating the role of the environment on specific cyclone features. It would be particularly interesting to perform idealised mesoscale simulations of these cyclogenesis events to examine the sensitivity to atmospheric conditions. Evidence of simulated Secondary+ cyclones has been demonstrated as an upstream response to the forcing of a Primary cyclone via an upper-level PV anomaly in some idealised channel simulations (Schemm et al., 2013). Furthermore, sensitivity experiments into drivers of the Primary and Secondary+ track orientation would also be an interesting avenue to pursue with the upper-level PV structure and moist processes being shown to be important for the poleward propagation of idealised mid-latitude cyclones (Coronel et al., 2015). Finally, the superposition of the polar and subtropical jet has been shown to be important for some cyclogenesis cases near the eastern coast of North America and in initiating a strengthening of the upper-level flow (Winters and Martin, 2017), therefore it would be of interest to explore how these superposition events affect the jet structure downstream and impact the formation of Primary cyclones in the vicinity of the superpositions.

Acknowledgements

Matthew D. K. Priestley is funded by NERC via the SCENARIO DTP (NE/L002566/1) and co-sponsored by Aon Impact Forecasting. Joaquim G. Pinto thanks the AXA Research fund for support. Len C. Shaffrey is funded by the ERA4CS WINDSURFER project and the National Centre for Atmospheric Science. We thank the ECMWF for their ERA-Interim Reanalysis (data available at https://apps.ecmwf.int/datasets).

Appendix A - Changes in Static Stability based on Thermal Wind Balance

Thermal Wind Balance formulated in terms of potential temperature (θ) in pressure (p) co-ordinates can be expressed as follows:

$$\frac{\partial u}{\partial p} = -\frac{1}{f\rho\theta}\left(\frac{\partial \theta}{\partial y}\right)_p \tag{A1}$$

Equation A1 can be simplified further by treating the Coriolis parameter (f), density (ρ), and the potential temperature (θ) as constant. Thereby giving:

$$\frac{\partial u}{\partial p} \approx -\left(\frac{\partial \theta}{\partial y}\right)_p \tag{A2}$$

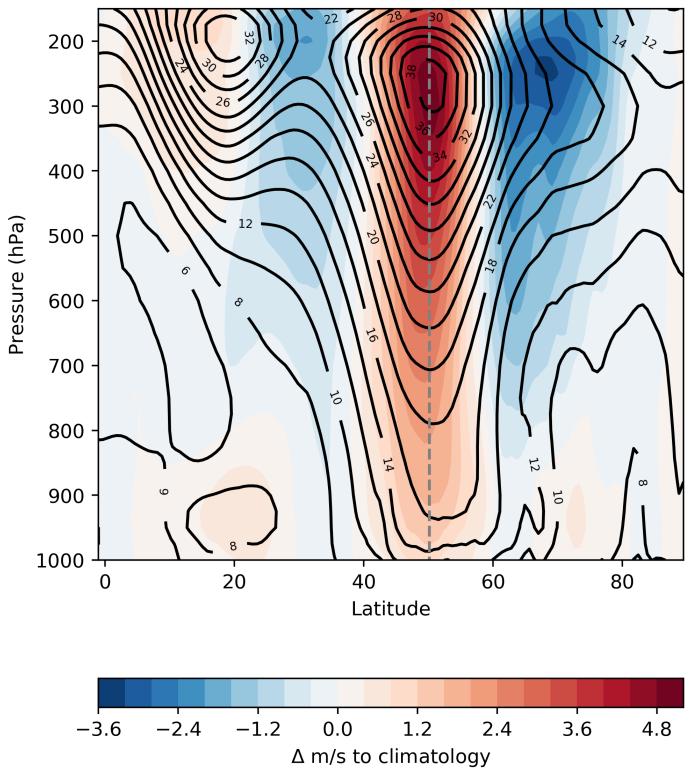

FIGURE A1 Composite image of zonal mean wind at the time of Secondary+ cyclogenesis for Secondary+ cyclones passing through 55°N. Zonal mean from 40-0°W. Black contours are the full field at the time of cyclogenesis and the coloured filled contours are the anomalies relative to the long-term climatology in m s^{-1}. The grey dashed line represents the mid-latitude jet axis.

In equation 1, the low-level static stability is formulated in pressure co-ordinates. By treating p, g, R, T, and $\bar{\theta}$ as approximately constant, this can be expressed as:

$$N^2 \approx \frac{\partial \theta}{\partial p} \tag{A3}$$

Through differentiating equation A2 with respect to p, the following relationship is obtained:

$$\frac{\partial^2 u}{\partial p^2} \approx -\frac{\partial}{\partial p}\left(\frac{\partial \theta}{\partial y}\right)_p \approx -\frac{\partial^2 u}{\partial p \partial y} \approx -\frac{\partial}{\partial y}\left(\frac{\partial \theta}{\partial p}\right) \tag{A4}$$

...ng the relationship in equation A3 substituted into equation A4 it therefore states that as the second derivative of u with respect to p increases, the meridional gradient of the static stability will become more negative.

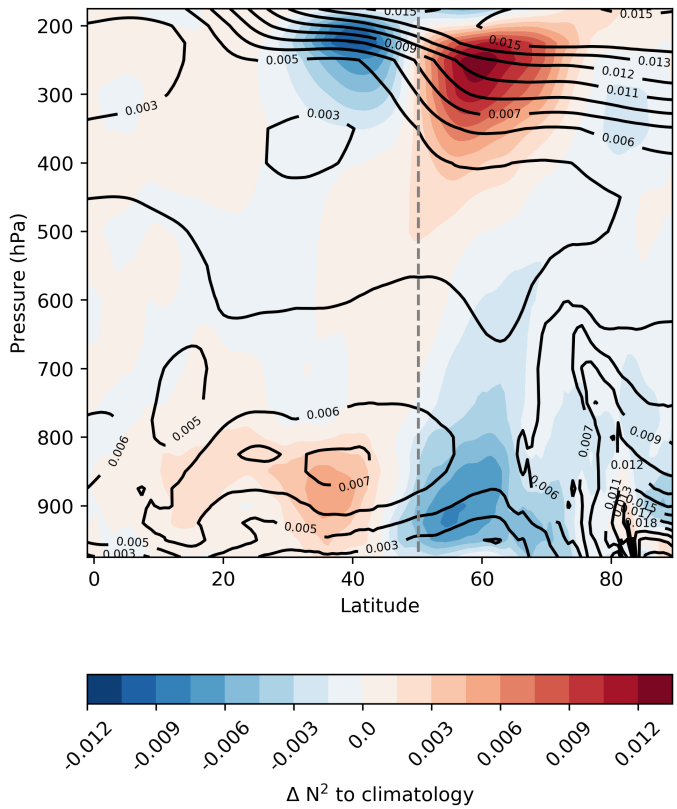

FIGURE A2 Composite image of zonal mean static stability (N^2) at the time of Secondary+ cyclogenesis for Secondary+ cyclones passing through 55°N. Zonal mean from 40-0°W. Black contours are the full field at the time of cyclogenesis and the coloured filled contours are the anomalies relative to the long-term climatology. The grey dashed line represents the mid-latitude jet axis.

From figure A1 it can be seen that the anomalies in the jet are throughout the depth of the atmosphere with a peak between 200 and 350 hPa. These changes in jet speed with height imply that the value of $\frac{\partial u}{\partial p}$ will be positive below the jet maximum and have a value of zero at the height of the jet core and then being negative above this. The maxima in $\frac{\partial u}{\partial p}$ will subsequently be in the middle troposphere. Through equation A2 this tells us that the gradient of θ will be increasing more across the jet in a northerly direction.

As $\frac{\partial u}{\partial p}$ will have a positive gradient in the lower troposphere, and a negative gradient in the upper troposphere this tells us that through equation A4 that $\frac{\partial^2 u}{\partial p^2}$ will be positive in the lower troposphere, negative in the upper troposphere, and have its minimum at the height of the jet maximum. The large values of $\frac{\partial^2 u}{\partial p^2}$ in the lower troposphere relate to a strong negative meridional N^2 (through equation A4) and the large negative values at the height of the jet maximum result in a positive meridional gradient of N^2 at that height. These patterns are seen in figure A2 with the stability gradients across the jet peaking at lower and upper levels, with negative N^2 anomalies on the poleward flank of the jet below 800 hPa. Furthermore, the anomalies of N^2 in the upper-troposphere can be related to the large-scale RWB and the PV anomalies associated with them. The RWB on the poleward (equatorward) flank of the jet will be associated with positive (negative) PV anomalies. The positive (negative) PV anomalies therefore are related to positive (negative) anomalies of static stability within the anomaly itself due to the associated bending of the isentropes.

references

Adamson, D., Belcher, S. E., Hoskins, B. J., Plant, R. S. et al. (2006) Boundary-layer friction in midlatitude cyclones. *Quarterly Journal of the Royal Meteorological Society*, **132**, 101–124.

Barnes, E. A. and Hartmann, D. L. (2012) Detection of Rossby wave breaking and its response to shifts of the midlatitude jet with climate change. *Journal of Geophysical Research: Atmospheres*, **117**, 1–17.

Bell, G. D. and Bosart, L. F. (1989) The large-scale atmospheric structure accompanying new england coastal frontogenesis and associated north american east coast cyclogenesis. *Quarterly Journal of the Royal Meteorological Society*, **115**, 1133–1146.

Berry, G., Reeder, M. J. and Jakob, C. (2011) A global climatology of atmospheric fronts. *Geophysical Research Letters*, **38**, L04809.

Bishop, C. H. and Thorpe, A. J. (1994a) Frontal wave stability during moist deformation frontogenesis. part i: Linear wave dynamics. *Journal of the Atmospheric Sciences*, **51**, 852–873.

— (1994b) Frontal wave stability during moist deformation frontogenesis. part ii: The suppression of nonlinear wave development. *Journal of the Atmospheric Sciences*, **51**, 874–888.

Bjerknes, J. and Solberg, H. (1922) Life cycle of cyclones and the polar front theory of atmospheric circulation. *Geophysisks Publikationer*, **3**, 3–18.

Bosart, L. F. (1975) New england coastal frontogenesis. *Quarterly Journal of the Royal Meteorological Society*, **101**, 957–978.

Brayshaw, D. J., Hoskins, B. and Blackburn, M. (2009) The basic ingredients of the north atlantic storm track. part i: Land–sea contrast and orography. *Journal of the Atmospheric Sciences*, **66**, 2539–2558.

— (2011) The basic ingredients of the north atlantic storm track. part ii: Sea surface temperatures. *Journal of the Atmospheric Sciences*, **68**, 1784–1805.

Catto, J. L. and Pfahl, S. (2013) The importance of fronts for extreme precipitation. *Journal of Geophysical Research: Atmospheres*, **118**, 10,791–10,801.

Chaboureau, J. and Thorpe, A. J. (1999) Frontogenesis and the development of secondary wave cyclones in fastex. *Quarterly Journal of the Royal Meteorological Society*, **125**, 925–940.

Coronel, B., Ricard, D., Rivière, G. and Arbogast, P. (2015) Role of moist processes in the tracks of idealized midlatitude surface cyclones. *Journal of the Atmospheric Sciences*, **72**, 2979–2996.

Davie, H. F. and Gray, S. L. (2006) Life-cycle simulations of shallow frontal waves and the impact of deformation strain. *Quarterly Journal of the Royal Meteorological Society*, **132**, 2171–2190.

— (2009) The spatial distribution and evolution characteristics of north atlantic cyclones. *Monthly Weather Review*, **137**, 99–115.

Davis, C. A. and Emanuel, K. A. (1991) Potential vorticity diagnostics of cyclogenesis. *Monthly Weather Review*, **119**, 1929–1953.

Dee, D., Uppala, S., Simmons, A., Berrisford, P., Poli, P., Kobayashi, S., Andrae, U., Balmaseda, M., Balsamo, G., Bauer, P. et al. (2011) The era-interim reanalysis: Configuration and performance of the data assimilation system. *Quarterly Journal of the Royal Meteorological Society*, **137**, 553–597.

Deveson, A. C. L., Browning, K. A. and Hewson, T. D. (2002) A classification of fastex cyclones using a height-attributable quasi-geostrophic vertical-motion diagnostic. *Quarterly Journal of the Royal Meteorological Society*, **128**, 93–117.

Economou, T., Stephenson, D. B., Pinto, J. G., Shaffrey, L. C. and Zappa, G. (2015) Serial clustering of extratropical cyclones in a multi-model ensemble of historical and future simulations. *Quarterly Journal of the Royal Meteorological Society*, **141**, 3076–3087.

Flocas, H. A., Simmonds, I., Kouroutzoglou, J., Keay, K., Hatzaki, M., Bricolas, V. and Asimakopoulos, D. (2010) On cyclonic tracks over the eastern mediterranean. *Journal of Climate*, **23**, 5243–5257.

Gomara, I., Pinto, J. G., Woollings, T., Masato, G., Zurita-Gotor, P. and Rodríguez-Fonseca, B. (2014) Rossby wave-breaking analysis of explosive cyclones in the euro-atlantic sector. *Quarterly Journal of the Royal Meteorological Society*, **140**, 738–753.

Gomara, I., Rodríguez-Fonseca, B., Zurita-Gotor, P. and Pinto, J. (2014) On the relation between explosive cyclones affecting Europe and the North Atlantic Oscillation. *Geophysical Research Letters*, **41**, 2182–2190.

Gray, S. L. and Dacre, H. F. (2006) Classifying dynamical forcing mechanisms using a climatology of extratropical cyclones. *Quarterly Journal of the Royal Meteorological Society*, **132**, 1119–1137.

Gyakum, J. R., Carrera, M., Zhang, D.-L., Miller, S., Caveen, J., Benoit, R., Black, T., Buzzi, A., Chouinard, C., Fantini, M., Folloni, C., Katzfey, J. J., Kuo, Y.-H., Lalaurette, F., Low-Nam, S., Mailhot, J., Malguzzi, P., McGregor, J. L., Nakamura, M., Tripoli, G. and Wilson, C. (1996) A regional model intercomparison using a case of explosive oceanic cyclogenesis. *Weather and Forecasting*, **11**, 521–543.

Hanley, J. and Caballero, R. (2012) The role of large-scale atmospheric flow and Rossby wave breaking in the evolution of extreme windstorms over Europe. *Geophysical Research Letters*, **39**, L21708.

Hewson, T. D. (1998) Objective fronts. *Meteorological Applications*, **5**, 37–65.

Hofstätter, M., Chimani, B., Lexer, A. and Blöschl, G. (2016) A new classification scheme of european cyclone tracks with relevance to precipitation. *Water Resources Research*, **52**, 7086–7104.

Hope, P., Keay, K., Pook, M., Catto, J., Simmonds, I., Mills, G., McIntosh, P., Risbey, J. and Berry, G. (2014) A comparison of automated methods of front recognition for climate studies: A case study in southwest western australia. *Monthly Weather Review*, **142**, 343–363.

Hoskins, B. and Berrisford, P. (1988) A potential vorticity perspective of the storm of 15–16 october 1987. *Weather*, **43**, 122–129.

Hoskins, B. J. and Hodges, K. I. (2002) New perspectives on the northern hemisphere winter storm tracks. *Journal of the Atmospheric Sciences*, **59**, 1041–1061.

Hoskins, B. J., McIntyre, M. E. and Robertson, A. W. (1985) On the use and significance of isentropic potential vorticity maps. *Quarterly Journal of the Royal Meteorological Society*, **111**, 877–946.

Joly, A. and Thorpe, A. J. (1990) Frontal instability generated by tropospheric potential vorticity anomalies. *Quarterly Journal of the Royal Meteorological Society*, **116**, 525–560.

Kuo, Y.-H., Gyakum, J. R. and Guo, Z. (1995) A case of rapid continental mesoscale cyclogenesis. part i: Model sensitivity experiments. *Monthly Weather Review*, **123**, 970–997.

Ludwig, P., Pinto, J. G., Hoepp, S. A., Fink, A. H. and Gray, S. L. (2015) Secondary cyclogenesis along an occluded front leading to damaging wind gusts: Windstorm kyrill, january 2007. *Monthly Weather Review*, **143**, 1417–1437.

Mailier, P. J., Stephenson, D. B., Ferro, C. A. T. and Hodges, K. I. (2006) Serial Clustering of Extratropical Cyclones. *Monthly Weather Review*, **134**, 2224–2240.

Masato, G., Hoskins, B. J. and Woollings, T. (2013) Wave-Breaking Characteristics of Northern Hemisphere Winter Blocking: A Two-Dimensional Approach. *Journal of Climate*, **26**, 4535–4549.

Messori, G. and Caballero, R. (2015) On double rossby wave breaking in the north atlantic. *Journal of Geophysical Research: Atmospheres*, **120**, 11,129–11,150.

Miller, J. E. (1946) Cyclogenesis in the atlantic coastal region of the united states. *Journal of Meteorology*, **3**, 31–44.

Murray, R. J. and Simmonds, I. (1991) A numerical scheme for tracking cyclone centres from digital data. Part I: Development and operation of the scheme. *Australian Meteorological Magazine*, **39**, 155–166.

Neu, U., Akperov, M. G., Bellenbaum, N., Benestad, R., Blender, R., Caballero, R., Cocozza, A., Dacre, H. F., Feng, Y., Fraedrich, K., Grieger, J., Gulev, S., Hanley, J., Hewson, T., Inatsu, M., Keay, K., Kew, S. F., Kindem, I., Leckebusch, G. C., Liberato, M. L. R., Lionello, P., Mokhov, I. I., Pinto, J. G., Raible, C. C., Reale, M., Rudeva, I., Schuster, M., Simmonds, I., Sinclair, M., Sprenger, M., Tilinina, N. D., Trigo, I. F., Ulbrich, S., Ulbrich, U., Wang, X. L. and Wernli, H. (2013) Imilast: A community effort to intercompare extratropical cyclone detection and tracking algorithms. *Bulletin of the American Meteorological Society*, **94**, 529–547.

Nielsen, J. W. (1989) The formation of new england coastal fronts. *Monthly Weather Review*, **117**, 1380–1401.

Papritz, L., Pfahl, S., Rudeva, I., Simmonds, I., Sodemann, H. and Wernli, H. (2014) The role of extratropical cyclones and fronts for southern ocean freshwater fluxes. *Journal of Climate*, **27**, 6205–6224.

Parker, D. J. (1998) Secondary frontal waves in the North Atlantic region: A dynamical perspective of current ideas. *Quarterly Journal of the Royal Meteorological Society*, **124**, 829–856.

Pearce, R., Lloyd, D. and McConnell, D. (2001) The post-christmas 'french' storms of 1999. *Weather*, **56**, 81–91.

Petterssen, S., Dunn, G. E. and Means, L. L. (1955) Report of an experiement in forecasting of cyclone development. *Journal of Meteorology*, **12**, 58–67.

Pinto, J. G., Gómara, I., Masato, G., Dacre, H. F., Woollings, T. and Caballero, R. (2014) Large-scale dynamics associated with clustering of extratropical cyclones affecting Western Europe. *Journal of Geophysical Research: Atmospheres*, **119**, 13,704–13,719.

Pinto, J. G., Spangehl, T., Ulbrich, U. and Speth, P. (2005) Sensitivities of a cyclone detection and tracking algorithm: individual tracks and climatology. *Meteorologische Zeitschrift*, **14**, 823–838.

Pinto, J. G., Ulbrich, S., Economou, T., Stephenson, D. B., Karremann, M. K. and Shaffrey, L. C. (2016) Robustness of serial clustering of extratropical cyclones to the choice of tracking method. *Tellus A: Dynamic Meteorology and Oceanography*, **68**, 32204.

Pinto, J. G., Zacharias, S., Fink, A. H., Leckebusch, G. C. and Ulbrich, U. (2009) Factors contributing to the development of extreme north atlantic cyclones and their relationship with the nao. *Climate dynamics*, **32**, 711–737.

Plant, R., Craig, G. C. and Gray, S. (2003) On a threefold classification of extratropical cyclogenesis. *Quarterly Journal of the Royal Meteorological Society*, **129**, 2989–3012.

Priestley, M. D. K., Pinto, J. G., Dacre, H. F. and Shaffrey, L. C. (2017a) The role of cyclone clustering during the stormy winter of 2013/2014. *Weather*, **72**, 187–192.

— (2017b) Rossby wave breaking, the upper level jet, and serial clustering of extratropical cyclones in western europe. *Geophysical Research Letters*, **44**, 514–521.

Raible, C. C., Della-Marta, P. M., Schwierz, C., Wernli, H. and Blender, R. (2008) Northern hemisphere extratropical cyclones: A comparison of detection and tracking methods and different reanalyses. *Monthly Weather Review*, **136**, 880–897.

Rivals, H., Cammas, J.-P. and Renfrew, I. A. (1998) Secondary cyclogenesis: The initiation phase of a frontal wave observed over the eastern atlantic. *Quarterly Journal of the Royal Meteorological Society*, **124**, 243–268.

Rivière, G. and Joly, A. (2006a) Role of the low-frequency deformation field on the explosive growth of extratropical cyclones at the jet exit. part i: Barotropic critical region. *Journal of the atmospheric sciences*, **63**, 1965–1981.

— (2006b) Role of the low-frequency deformation field on the explosive growth of extratropical cyclones at the jet exit. part ii: Baroclinic critical region. *Journal of the atmospheric sciences*, **63**, 1982–1995.

Rivière, G. and Orlanski, I. (2007) Characteristics of the atlantic storm-track eddy activity and its relation with the north atlantic oscillation. *Journal of the Atmospheric Sciences*, **64**, 241–266.

Schemm, S., Rudeva, I. and Simmonds, I. (2015) Extratropical fronts in the lower troposphere–global perspectives obtained from two automated methods. *Quarterly Journal of the Royal Meteorological Society*, **141**, 1686–1698.

Schemm, S. and Sprenger, M. (2015) Frontal-wave cyclogenesis in the north atlantic – a climatological characterisation. *Quarterly Journal of the Royal Meteorological Society*, **141**, 2989–3005.

Schemm, S., Sprenger, M. and Wernli, H. (2018) When during their life cycle are extratropical cyclones attended by fronts? *Bulletin of the American Meteorological Society*, **99**, 149–165.

Schemm, S., Wernli, H. and Papritz, L. (2013) Warm conveyor belts in idealized moist baroclinic wave simulations. *Journal of the Atmospheric Sciences*, **70**, 627–652.

Schär, C. and Davies, H. C. (1990) An instability of mature cold fronts. *Journal of the Atmospheric Sciences*, **47**, 929–950.

Simmonds, I., Keay, K. and Tristram Bye, J. A. (2012) Identification and climatology of southern hemisphere mobile fronts in a modern reanalysis. *Journal of Climate*, **25**, 1945–1962.

Thomas, C. M. and Schultz, D. M. (2019) What are the best thermodynamic quantity and function to define a front in gridded model output? *Bulletin of the American Meteorological Society*, **100**, 873–895.

Thorncroft, C. D., Hoskins, B. J. and McIntyre, M. E. (1993) Two paradigms of baroclinic-wave life-cycle behaviour. *Quarterly Journal of the Royal Meteorological Society*, **119**, 17–55.

Campa, J. and Wernli, H. (2012) A pv perspective on the vertical structure of mature midlatitude cyclones in the northern hemisphere. *Journal of the Atmospheric Sciences*, **69**, 725–740.

Uccellini, L. W., Petersen, R. A., Kocin, P. J., Brill, K. F. and Tuccillo, J. J. (1987) Synergistic interactions between an upper-level jet streak and diabatic processes that influence the development of a low-level jet and a secondary coastal cyclone. *Monthly Weather Review*, **115**, 2227–2261.

Vicente-Serrano, R., Stephenson, D. B., Cook, L. M. and Mitchell-Wallace, K. (2009) Serial clustering of intense European storms. *Meteorologische Zeitschrift*, **18**, 411–424.

Walz, M. A., Befort, D. J., Kirchner-Bossi, N. O., Ulbrich, U. and Leckebusch, G. C. (2018) Modelling serial clustering and interannual variability of european winter windstorms based on large-scale drivers. *International Journal of Climatology*, **38**, 3044–3057.

Wang, C.-C. and Rogers, J. C. (2001) A composite study of explosive cyclogenesis in different sectors of the north atlantic. part i: Cyclone structure and evolution. *Monthly Weather Review*, **129**, 1481–1499.

Wernli, H., Dirren, S., Liniger, M. A. and Zillig, M. (2002) Dynamical aspects of the life cycle of the winter storm 'lothar' (24–26 december 1999). *Quarterly Journal of the Royal Meteorological Society*, **128**, 405–429.

Wernli, H. and Schwierz, C. (2006) Surface cyclones in the era-40 dataset (1958–2001). part i: Novel identification method and global climatology. *Journal of the Atmospheric Sciences*, **63**, 2486–2507.

Whittaker, L. M. and Horn, L. H. (1984) Northern hemisphere extratropical cyclone activity for four mid-season months. *Journal of Climatology*, **4**, 297–310.

Winters, A. C. and Martin, J. E. (2017) Diagnosis of a north american polar–subtropical jet superposition employing piecewise potential vorticity inversion. *Monthly Weather Review*, **145**, 1853–1873.